with Linear Predictor for Systems with Dead Time," *Electron. Lett.*, 7, No. 12, 335-337 (1971*a*).

———, "State-Feedback Controller for Systems with Dead Time," *ibid.*, No. 5/6, 131-133 (1971*b*).

Lupfer, D. E., and M. W. Oglesby, "Applying Dead-Time Compensation for Linear Predictor Process Control," *ISA Journal*, 8, No. 11, 53-57 (1961).

———, "The Application of Dead-Time Compensation to a Chemical Reactor for Automatic Control of Production Rate," *ISA Trans.*, 1, 72-80 (1962).

Marshall, J. E., "Extension of O. J. Smith's Method to Digital and Other Systems," *Int. J. Control*, 19, 933-939 (1974).

Mee, D. H., "An Extension of Predictor Control for Systems with Control Time Delays," *ibid.*, 18, 1151-1168 (1973).

Meyer, C., "Experimental Evaluation of Predictor Control Schemes for Distillation Column Control," M.Sc. thesis, Univ. Alberta, Edmonton, Canada (1977).

———, D. E. Seborg, and R. K. Wood, "A Comparison of the Smith Predictor and Conventional Feedback Control," *Chem. Eng. Sci.*, 31, 775-778 (1976).

———, "An Experimental Application of Time Delay Compensation Techniques to Distillation Column Control," *Ind. Eng. Chem. Process Develop.*, 17, 62-67 (1978).

Mollenkamp, R. A., C. L. Smith, and A. B. Corripio, "Designing Digital Controllers for Fast Processes," *Instr. Control Systems*, 46, No. 8, 47-49 (1973).

Moore, C. F., "Selected Problems in the Design and Implementation of Direct Digital Control," Ph.D. thesis La. State Univ. (1969).

———, C. L. Smith, and P. W. Murrill, "Improved Algorithm for Direct Digital Control," *Instr. Control Systems*, 43, No. 1, 70-74 (1970).

———, "Simplifying Digital Control Dynamics for Controller Tuning and Hardware Lag Effects," *Instr. Pract.*, No. 1, 45-49 (1969).

Nielsen, G., "Control of Systems with Time Delay," *Proc. Fourth IFAC Congress*, Warsaw (1969).

Pacey, W. C., "Control of a Binary Distillation Column," M.Sc. thesis, Univ. Alberta, Edmonton, Canada (1973).

Prasad, C. C., and P. R. Krishnaswamy, "Control of Pure Time Delay Processes," *Chem. Eng. Sci.*, 30, 207-215 (1975).

Rademaker, O., J. E. Rijnsdorp, and A. Maarleveld, *Dynamics and Control of Continuous Distillation Units*, Elsevier, New York (1975).

Shinskey, F. G., *Distillation Control for Productivity and Energy Conservation*, McGraw-Hill, New York (1977).

Smith, C. A., and F. R. Groves, "Dead Time Compensation Based on Empirical Nonlinear Process Models," *Proc. 28th Ann. ISA Conf.*, Houston, Tex. (1973).

Smith, O. J. M., "A Controller to Overcome Dead Time," *ISA Journal*, 6, No. 2, 28-33 (1959).

———, "Closer Control of Loops with Dead Time," *Chem. Eng. Progr.*, 53, No. 5, 217-219 (1957).

Svrcek, W. Y., "Dynamic Response of a Binary Distillation Column," Ph.D. thesis, Univ. Alberta, Edmonton, Canada (1967).

Tong, R., "Self-tuning Regulator Control of a Binary Distillation Column," M.Sc. thesis, Univ. Alberta, Edmonton, Canada (Expected completion, 1979).

Wood, R. K., and M. W. Berry, "Terminal Composition Control of a Binary Distillation Column," *Chem. Eng. Sci.*, 28, 1707-1717 (1973).

Manuscript received July 18, 1977; revision received July 10, and accepted July 18, 1978.

An Experimental Study of the Rheological Behavior of Surface Films

A constitutive equation has been developed to relate surface stresses to the deformational history of an interface. To verify the applicability of the equation to real surface films, experimental studies involving spread and adsorbed monolayers have been conducted using the deep-channel surface rheometer operated both under the conditions of oscillatory and constant floor motion. The results reported here are the first obtained using an oscillatory system.

Experimental results indicate that both spread and adsorbed monolayers can exhibit viscoelastic behavior which may be represented by the model. Furthermore, it has been found that for three long chain, fatty acid films, spread on a *p*H 6.1 aqueous substrate, surface shear viscosity and surface elasticity increase with film pressure and molecular weight. The observed rheological behavior was found to be strongly *p*H dependent.

J. V. ADDISON
and
R. S. SCHECHTER

Department of Chemical Engineering
The University of Texas at Austin
Austin, Texas 78712

SCOPE

An interfacial constitutive equation has been proposed (Gardner et al., 1977) which allows for both non-Newtonian steady shear and viscoelastic behavior and thus provides a unified description of complex interfacial phenomena. The objective of this study is to verify the applicability of this constitutive equation and associated models to real surface films. In order to achieve this, rheological experiments have been conducted with spread films of long chain, fatty acids and an adsorbed polymeric film using the deep-channel surface rheometer (Gardner et al., 1977; Burton and Mannheimer, 1967; Mannheimer and Schechter, 1970). In order to evaluate the parameters associated with the proposed constitutive equation, a new experimental technique which employs a small amplitude sinusoidal deformation has been used in conjunction with surface viscometry.

0001-1541-79-1896-0032-$01.15.

CONCLUSIONS AND SIGNIFICANCE

It has been found that the deep-channel surface rheometer may be used to analyze complex rheological behavior of spread and adsorbed surface films. Of particular significance is the applicability of the general surface constitutive equation and resulting surface rheological models in describing viscoelastic interfaces.

Experimental results indicate that films of long-chain, fatty acids spread on an aqueous substrate of *p*H 6.1 are viscoelastic. Furthermore, it was found that surface shear viscosity (η_0, η_∞, η') and surface rigidity (η'') increase with film pressure and molecular weight.

Substrate *p*H was found to affect the rheological behavior of spread fatty acid films. In particular, it was found that an arachidic acid film spread on a *p*H 6.1 substrate behaved as a Newtonian film of very low surface viscosity. The behavior at *p*H 6.1 may be due to the formation of soaps formed by the interaction of the carboxylate anions with trace amounts of multivalent cations present in the substrate.

A study of the limitations of the surface viscometer (constant floor motion) indicates that if no film is present at the interface, the device must be operated so that $\Omega_{max} \leq 45$ deg/s for D between ~ 0.15 and ~ 0.20 or $\Omega_{max} \leq 30$ deg/s for $D \approx 0.26$ to avoid secondary surface flows. However, if the infinite shear rate surface viscosity η_∞ is greater than $\sim 3 \times 10^{-6}$ kg/s, it appears that Ω may be as large as 70 deg/s (for $D \approx 0.2$) before secondary flows have an influence.

The oscillatory surface rheometer, while useful for determining relaxation times for the films studied, is limited to films characterized by parameters such that $\eta_\infty << \eta_0 < 10^{-3}$ kgk/s and $\lambda > 0.5$ s. In addition, the lower limit for D (which corresponds to the maximum shear rate obtainable) was found to be approximately 0.15.

The sensitivity of the experimentally determined parameters to the depth of fluid in the canal (or D) was tested by performing the viscometric and oscillatory experiments at different values of D. It was found that the two parameter sets differed by approximately 10%.

Viscoelastic behavior was also characteristic for adsorbed films of poly(vinyl-alcohol). The observed transition floor rotation rate, however, was greater than for the fatty acids by at least a factor of two, which may be due to a higher degree of molecular entanglements in the poly(vinyl-alcohol) film.

Time dependent rheological behavior has been observed for poly(vinyl-alcohol) of 115 000 molecular weight in which the transition floor speed (which, in this case, may be related to a yield stress) and η_∞ increase with time and approach a limiting value. This phenomenon is mostly likely due to a slow surface diffusion rate for poly(vinyl-alcohol) molecules where the surface concentration slowly increases, approaching an equilibrium value.

A RHEOLOGICAL MODEL FOR VISCOELASTIC INTERFACES

The constitutive equation used here to describe interfacial rheological behavior is a modified, two-dimensional version of a constitutive equation proposed by Tanner and Simmons (1967) for incompressible viscoelastic bulk phases. The model has been modified (Gardner, 1975) to apply to viscoelastic interfaces and is not limited to incompressible interfaces.

The surface film is presumed to be characterized by a memory function $m(s)$. The general equation will not be described here, but the results as applied to certain special cases of experimental interest will be presented.

Steady Shear Surface Flows

Consider a flat interface lying in the $x - y$ plane of a Cartesian coordinate system x, y, z. Suppose that the interface is undergoing a steady shear such that

$$V_y = 0 \tag{1}$$

and

$$V_x = V_x(y) \tag{2}$$

The surface stress is given by

$$\tau^s_{xy} = \eta(\dot{\gamma}) \left| \frac{dV_x}{dy} \right| \tag{3}$$

where the material function $\eta(\dot{\gamma})$ (or surface shear viscosity) is

$$\eta(\dot{\gamma}) = \int_0^{B/\dot{\gamma}} s\, m(s) ds \tag{4}$$

and is a function of $\dot{\gamma}$, the interfacial shear rate:

$$\dot{\gamma} = \left| \frac{dV_x}{dy} \right| \tag{5}$$

B is a parameter which indicates the magnitude of deformation necessary to cause the film to lose its memory.

An approximate expression for the memory function has been proposed (1) (2) as

$$m(s) = \frac{\delta(s)}{s} \eta_\infty + \sum_{n=1}^{\infty} \frac{\mu_n}{\lambda_n^2} e^{-s/\lambda_n} \tag{6}$$

where

$$\mu_n = (\eta_0 - \eta_\infty) \frac{\left(\dfrac{2}{n+1}\right)^\alpha}{\displaystyle\sum_{p=1}^{\infty} \left(\dfrac{2}{p+1}\right)^\alpha}$$

$$\lambda_n = \lambda \left(\frac{2}{n+1}\right)^\beta \tag{7}$$

Equations (6) and (7) are similar to those proposed by Bird and Carreau (1968). The parameters α, β, η_0, η_∞, and λ are discussed in subsequent sections.

Small Deformational Sinusoidal Shear Surface Flows

Again, consider a flat interface in the $x - y$ plane of the Cartesian coordinate system, but now suppose that the interface is undergoing a small amplitude, sinusoidal shear such that

$$V_x = Im\, \{V^* e^{i\omega t}\} \tag{8}$$

and

$$V_y = 0 \tag{9}$$

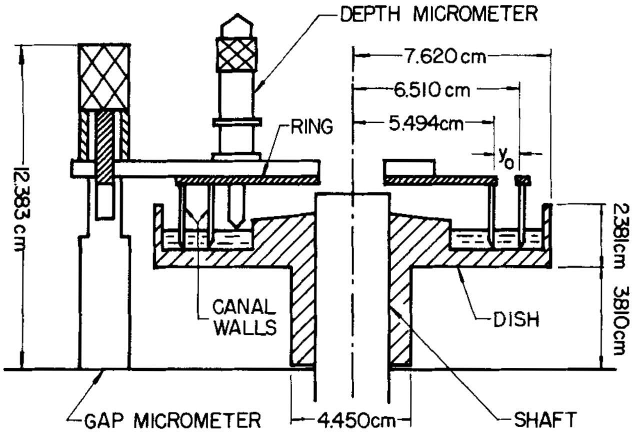

Fig. 1. The deep-channel surface rheometer.

The interfacial shear stress (Gardner and Schechter, 1976) is

$$\tau^s_{xy} = - Im \left\{ \eta^*(\omega) \frac{dV^*}{dy} e^{i\omega t} \right\} \tag{10}$$

and if the amplitude of oscillation is sufficiently small (Gardner et al., 1977)

$$\tau^s_{xx} = - \tau^s_{yy} \doteq 0 \tag{11}$$

where

$$\eta^*(\omega) = \eta' - i\left(\frac{G'}{\omega}\right) \tag{12}$$

$$\eta'(\omega) = \int_0^\infty \frac{m(s)\sin(\omega s)ds}{\omega} \tag{13}$$

$$G'(\omega) = \int_0^\infty m(s)[1 - \cos(\omega s)]ds \tag{14}$$

The dynamic surface viscosity η' is the in-phase component of the complex surface viscosity η^* and represents the viscous component of η^*. The out-of-phase term G'/ω represents the elastic component of η^*. Note that for a purely viscous interface, $G' = 0$, and for a purely elastic interface, $\eta' = 0$ (Gardner et al., 1977).

Material Functions

Note that the material functions $\eta(\dot\gamma)$, $\eta'(\omega)$ and $G'(\omega)$ are all related through the memory function $m(s)$ [Equation (6)]. After integration of Equations (4), (13), and (14), the material functions become

$$\eta(\dot\gamma) = \eta_\infty + \sum_{n=1}^{\infty} \mu_n \left\{ 1 - \left(1 + \frac{B}{\lambda_n \dot\gamma} \right) e^{-B/\lambda_n \dot\gamma} \right\} \tag{15}$$

$$\eta'(\omega) = \eta_\infty + \sum_{n=1}^{\infty} \frac{\mu_n}{1 + (\lambda_n \omega)^2} \tag{16}$$

$$\eta''(\omega) = G'(\omega)/\omega = \omega \sum_{n=1}^{\infty} \frac{\mu_n \lambda_n}{1 + (\lambda_n \omega)^2} \tag{17}$$

The surface shear viscosity function defined by Equation (15) is appropriate for describing shear thinning, viscoelastic interfaces under the condition of steady shear. In particular, note that as the magnitude of the shear rate $\dot\gamma$ increases to infinity, the function approaches a constant equal to η_∞ (the infinite shear rate surface viscosity). For $\dot\gamma$ approaching zero, the shear viscosity approaches η_0 (the zero shear rate surface viscosity). The rate at which these limiting values are attained is governed principally by the grouping B/λ, and to a lesser extent by α and β.

THE DEEP-CHANNEL SURFACE RHEOMETER

Figure 1 illustrates the design of the deep-channel surface rheometer. The device consists basically of a moving floor bounded by two fixed walls forming a canal. Its operation has been discussed in previous work (Burton and Mannheimer, 1967; Mannheimer and Schechter, 1970). Two types of floor motion are considered here, continuous rotation and small amplitude oscillation. The results presented in this paper are the first to be reported using an oscillatory floor. The application of this mode of operation will become evident.

Although the geometry of the canal assembly is annular, it has been shown that the assumption of a linear geometry is valid provided the rheometer is properly designed (Mannheimer, 1968). Furthermore, under certain conditions, the interface may be considered flat; that is, the meniscus may be neglected (Pintar et al., 1971).

Experimental Limitations of the Surface Rheometer

The primary limitation of the deep-channel surface viscometer (constant floor motion) is that there is an upper limit on the allowable shear rate magnitude, since secondary surface flows may arise causing a marked deviation from predicted theoretical behavior.

Gardner and Schechter (1976) have characterized this behavior by measuring the period of the floor (T_f) and that of the surface (T_p) as a function of the rotational speed (Ω) for the case where no film is present at the interface. Deviations from predicted behavior become evident when the period ratio shows a dependence on the floor rotation speed. In this work, the same approach was used for analyzing the influence of secondary flows, but the values for the depth parameter D were considerably smaller than in the previous study. Figure 2 shows T_f/T_p vs. Ω curves for three values of the depth to width ratio D for the case where no film is present. Note that the magnitude of the surface shear rate may be increased by either decreasing D or by increasing Ω.

For $D = 0.2600$, secondary flow apparently becomes important around $\Omega = 30$ deg/s. For $D = 0.2050$ and $D = 0.1501$, the deviation from theory occurs at higher values of 40 and 50 deg/s, respectively. (Data taken at $D = 0.1237$ were found to be unreproducible; hence, such a low value is not recommended.) So it appears that the maximum allowable shear rate in the absence of a film is defined by $D \doteq 0.15$ and $\Omega \doteq 40$ deg/s. Note

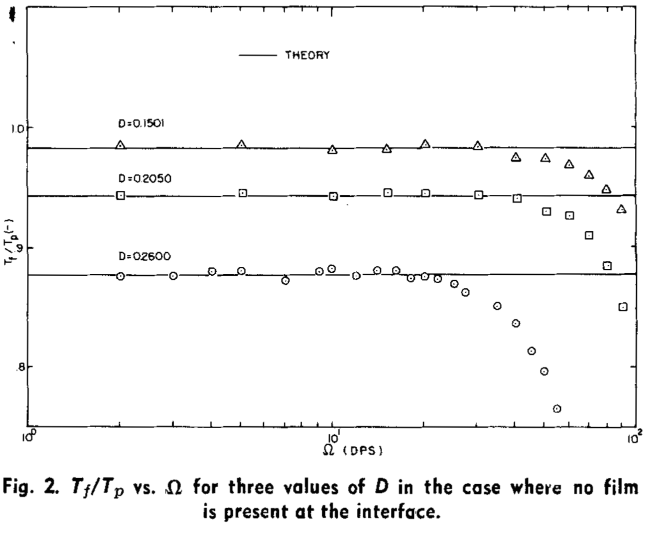

Fig. 2. T_f/T_p vs. Ω for three values of D in the case where no film is present at the interface.

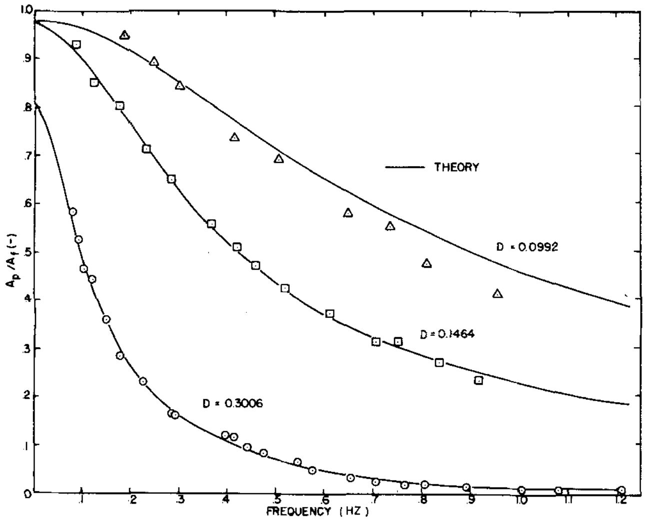

Fig. 3. A_p/A_f vs. frequency for three values of D in the case where no film is present at the interface.

that the shear rate at which secondary surface flows become evident for $D = 0.2600$ is much smaller than for either $D = 0.1501$ or $D = 0.2050$, which suggests that the depth of the hypophase as well as the shear rate magnitude are influential in creating secondary surface flows. This means that the upper and lower bounds of the operational constraints for the surface viscometer must be expressed in terms of both D and Ω and not in terms of $\dot{\gamma}$ alone. Hence, in the absence of a film, the operational constraints are such that at $D \doteq 0.26$, $\Omega_{\max} \doteq 30$ deg/s, whereas at $D \doteq 0.15$, $\Omega_{\max} \doteq 40$ deg/s.

In the viscometric experiment, D was approximately equal to 0.2 in all cases, so that the upper limit for floor rotation speed was 40 deg/s. However, this upper limit was exceeded for some cases in which films were present to determine $(T_f/T_p)_\infty$. It was assumed that if the surface was sufficiently viscous, secondary flows produced at the higher floor speeds would be damped out. Evidence will be presented to support this contention.

The primary limitation in the oscillatory rheometer experiment is due to the fact that some surface films possess such high surface viscosities that it is difficult to measure the amplitude of the oscillations accurately. However, this difficulty in measuring small amplitude ratios may be alleviated to some extent by decreasing the depth-to-width parameter D. But, as in the steady shear experiment, there is a lower limit on D. Figure 3 shows the relative amplitude of oscillation of the surface (A_p/A_f) vs. frequency for three values of D, wherein no film is present at the interface. For $D = 0.3006$ and $D = 0.1464$, there is good agreement with the theoretical predictions (solid lines); however, there is a marked deviation for $D = 0.0992$ which is perhaps caused by the gap between the canal walls and dish. The value of D used in this work was 0.2 and was found to be sufficient for the films studied.

EXPERIMENTAL

The stainless steel canal and dish assembly for the surface viscometer used in this study is shown in Figure 1. The canal walls and beveled edges are precisely machined so that the maximum eccentricity is ±0.0015 cm. The dish is secured on the motor shaft, and the gap between the beveled canal edges and the floor of the dish may be adjusted by use of three micrometers. The canal-and-dish assembly is isolated from the environment by a glass bubble which is fitted with a microscope.

The motor shaft is connected to a Genisco model C181 rate-of-turn table which provides variable rotation speeds from 0.001 to 1 200 deg/s.

The canal-and-dish design for the oscillatory rheometer is essentially the same as the steady shear rheometer, except that the gap between the canal walls is 0.85 cm. The oscillatory floor motion is induced by means of a sinusoidally oscillating bar connected to the drive shaft. The bar in turn is driven by a dc motor and an offset cam assembly. The motor drive for the oscillatory rheometer consists of an Electro-Craft model E-550 MGHP motor and corresponding speed regulator (model E-550M). The motor speed is infinitely variable over a 1 000:1 speed range which corresponds to a frequency range from ~0.01 to 1.7 Hz.

The oscillatory rheometer is also protected from the environment by a glass bubble fitted with a microscope. In addition, it is shielded from light by use of a hood. It was found that room light could induce convective currents in the surface rheometer, causing a particle at the surface centerline to migrate in the canal. To eliminate this difficulty and also to be able to observe the particle, a strobe light was used for illumination. The strobe light, with its short flash duration, produced little heat and did not cause the particle to migrate.

The environment inside the bubble was maintained at relatively high humidity by use of water-wet wicks. The temperature was not controlled and varied (23 ± 1°C).

The filling procedure insures that the contact angle between the substrate and the canal walls will be an advancing contact angle and hence will be large; therefore, the interface will be as flat as possible (Addison, 1977).

The rheological behavior of three spread films and one adsorbed film was studied in this work. The three spread films used were long chain fatty acids: tetradecanoic acid [$CH_3(CH_2)_{12}COOH$], stearic acid [$CH_3(CH_2)_{16}COOH$], and Arachidic acid [$CH_3(CH_2)_{18}COOH$]. The adsorbed films studied were 88% hydrolyzed poly(vinyl-alcohol) of 10 000 molecular weight and 100% hydrolyzed poly(vinyl-alcohol) of 115 000 molecular weight.

Tetradecanoic acid (M.W. = 228.38, m.p. = 52.5°C) was obtained from Eastman Kodak Company, stearic acid (M.W. = 284.49, m.p. = 69.6°C) from Fisher Scientific Company, arachidic acid (M.W. = 312.54, m.p. = 77.0°C) from K & K Laboratories, and poly(vinyl-alcohol) from Aldrich Chemical Company. All compounds used were of reagent grade.

The spreading solvent used was purified n-hexane. This reagent grade solvent was purified and dried by passing it through a silica gel column and storing over 4Å molecular sieves. The drying step is of the utmost importance, since trace amounts of water dissolved in the spreading solutions were found to drastically reduce their spreading ability. The concentration of each spreading solution was 0.2 kg/m^3.

The films were spread on distilled water (pH = 6.1) by means of a Hamilton microsyringe (10 μl capacity). The spreading technique consisted of carefully placing a number of 2 μl portions on the surface at various locations in the canal. The 2 μl portions were spread at 3 min intervals to allow the solvent to evaporate.

After the films were spread, a small Teflon particle (diameter ~0.01 cm) was placed on the surface, and the film was

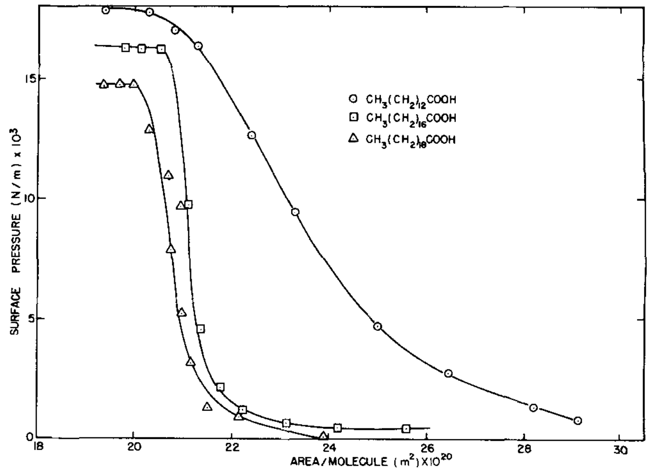

Fig. 4. Surface pressure vs. molecular area for C-14, C-18, and C-20 long chain fatty acids.

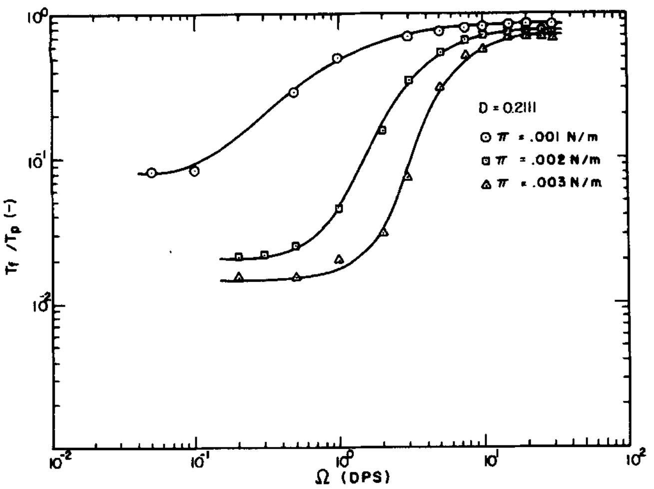

Fig. 5. T_f/T_p vs. Ω for a tetradecanoic acid (C-14) film spread on a pH 6.1 aqueous substrate at $\pi = 0.001$, 0.002, and 0.003 N/m.

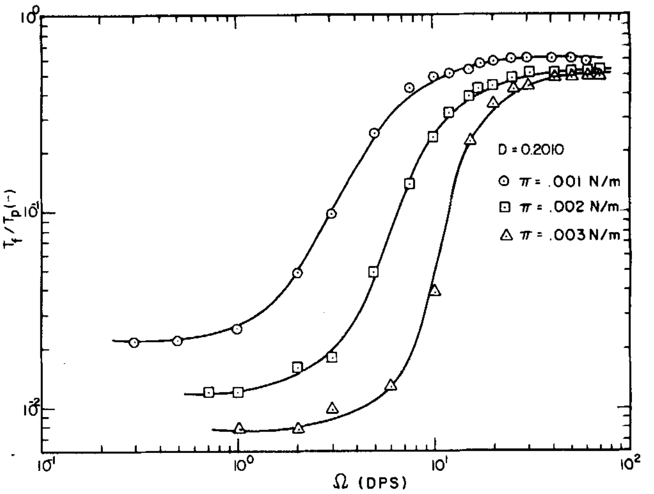

Fig. 6. T_f/T_p vs. Ω for a stearic acid (C-18) film spread on a pH 6.1 aqueous substrate at $\pi = 0.001$, 0.002, and 0.003 N/m.

allowed to equilibrate. The film is considered to be at equilibrium when the period ratio at some fixed value of floor rotation speed is constant with respect to time. Equilibration times for the three spread films was always less than 10 min; however, the adsorbed film of poly(vinyl-alcohol) required at least 8 hr to equilibrate owing to a slow surface diffusion rate.

Surface pressure vs. molecular area isotherms for the three fatty acids are shown in Figure 4. Film pressures were measured by the Wilhelmy plate method. The tensiometer used here consisted of a 5.5 cm long roughened platinum plate suspended from a Federal precision balance.

Film pressures measured using the technique outlined above were found to be reproducible to within ±0.0002 n/m.

Note that the π-A isotherms of Figure 4 were not generated by mechanically compressing the films but rather by increasing the surface concentration by applying increasing amounts of spreading solution. Trends similar to those illustrated in Figure 4 have been observed for mechanically compressed fatty acid films on aqueous substrates of various pH (Jarvis, 1965; Spink and Sanders, 1955).

RESULTS AND DISCUSSION

Experimentally Determined Parameters for Three Long Chain, Fatty Acid Spread Films

Each long chain fatty acid was spread on a pH 6.1 aqueous substrate at three surface pressures: 0.001, 0.002, and 0.003 n/m. The two surface rheological experiments were conducted for each acid to determine how the model parameters vary with film pressure and fatty acid molecular weight.

Figures 5, 6, and 7 show T_f/T_p vs. Ω data for the three fatty acids at the three film pressures. For a tetradecanoic acid film at $\pi = 0.001$ N/m ($A = 2.83 \times 10^{-19}$ m²/molecule), the rheological behavior is Newtonian ($\eta = \eta_0$) up to $\Omega \doteq 0.1$ deg/s. Then, T_f/T_p increases rapidly with Ω, indicating a transition to non-Newtonian behavior. For $\Omega > 30$ deg/s, T_f/T_p approaches a limiting value with $\eta = \eta_\infty < \eta_0$. The same trends are observed at $\pi = 0.002$ and $\pi = 0.003$ n/m. Note that $(T_f/T_p)_0$ and $(T_f/T_p)_\infty$ decrease with increasing film pressure π, and that the transition floor rotation rate increases (or, equivalently, B/λ increases) with increasing film pressure. This same trend occurs with spread stearic acid and arachidic acid films (Figures 6 and 7).

The data were fit by use of the six-parameter model. The limiting surface shear viscosities η_0 and η_∞ were determined by trial-and-error solution using experimental $(T_f/T_p)_0$ and $(T_f/T_p)_\infty$ data. The surface shear viscosity described by Equation (15) is, relatively speaking, not sensitive to α and β. In order to simplify the analysis of experimental data and to illustrate trends more clearly, α and β were both set equal to 2. This value represents the average value for α and β obtained from the oscillatory experiment. B/λ was determined so that the calculated T_f/T_p vs. Ω curves closely approximated the experimental data. These curves are shown in Figures 5, 6, and 7 for the C-14, C-18, and C-20 fatty acids, respectively.

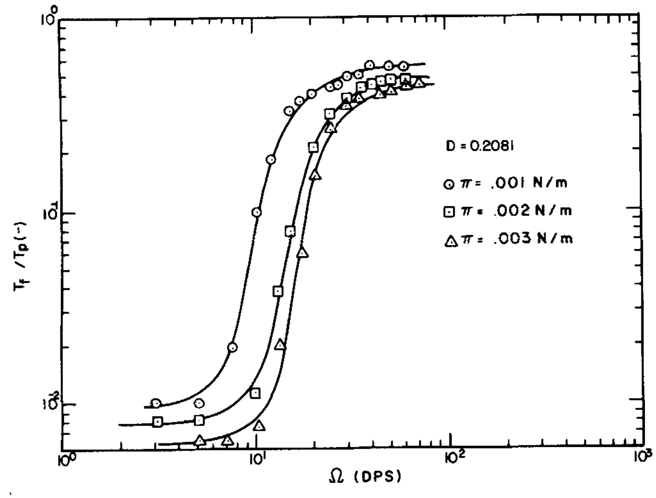

Fig. 7. T_f/T_p vs. Ω for an arachidic acid (C-20) film spread on a pH 6.1 aqueous substrate at $\pi = 0.001$, 0.002, and 0.003 N/m.

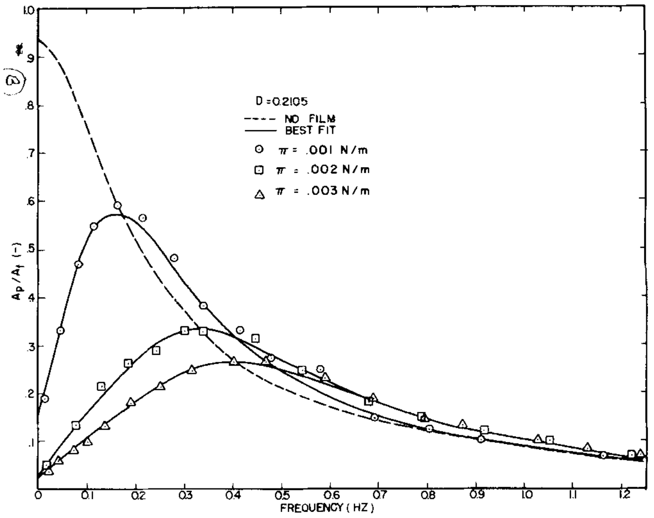

Fig. 8. A_p/A_f vs. frequency for a tetradecanoic acid fim spread on a pH 6.1 aqueous substrate at $\pi = 0.001$, 0.002, and 0.003 N/m.

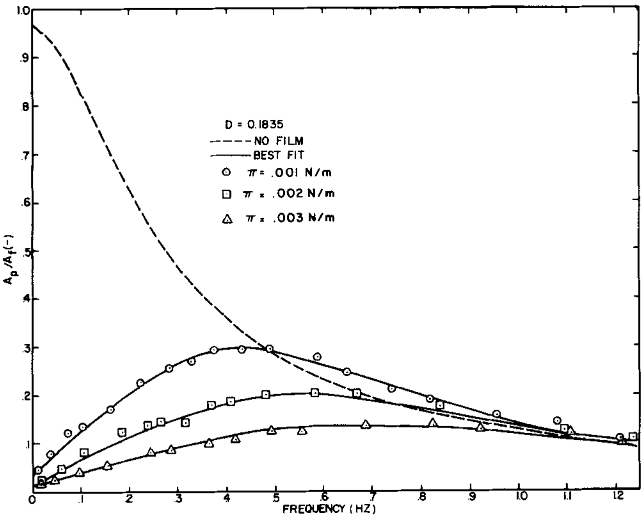

Fig. 9. A_p/A_f vs. frequency for a stearic acid film spread on a pH 6.1 aqueous substrate at $\pi = 0.001, 0.002,$ and 0.003 N/m.

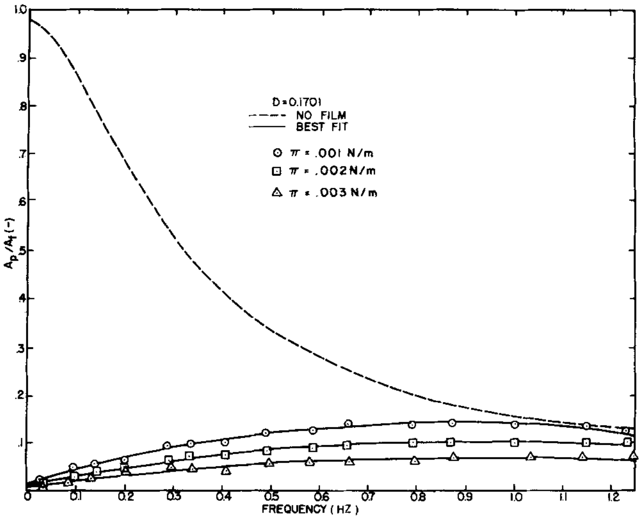

Fig. 10. A_p/A_f vs. frequency for an arachidic acid film spread on a pH 6.1 aqueous substrate at $\pi = 0.001, 0.002,$ and 0.003 N/m.

TABLE 1. EXPERIMENTALLY DETERMINED PARAMETERS

Film	π(N/m) × 10^3	η_0 (kg/s) × 10^3	η_∞ (kg/s) × 10^6	$B/\lambda(s^{-1})$	$B(-)$	$\lambda(s)$
Tetradecanoic acid	1	0.0625	0.9145	0.0058	0.5916	102.00
Tetradecanoic acid	2	0.2520	1.770	0.0080	0.7264	90.80
Tetradecanoic acid	3	0.3720	2.250	0.0088	0.7770	88.30
Stearic acid	1	0.2870	3.860	0.0121	0.7926	65.50
Stearic acid	2	0.4820	5.430	0.0133	0.7820	58.80
Stearic acid	3	0.7400	6.260	0.0163	0.8134	49.90
Arachidic acid	1	0.5700	4.680	0.091	0.9564	50.10
Arachidic acid	2	0.7200	6.650	0.249	0.9711	39.00
Arachidic acid	3	0.8800	7.000	0.0320	0.9760	30.50
PVA (M.W. = 10 000)	—	0.0550	9.910	1.8773	15.0000	7.99

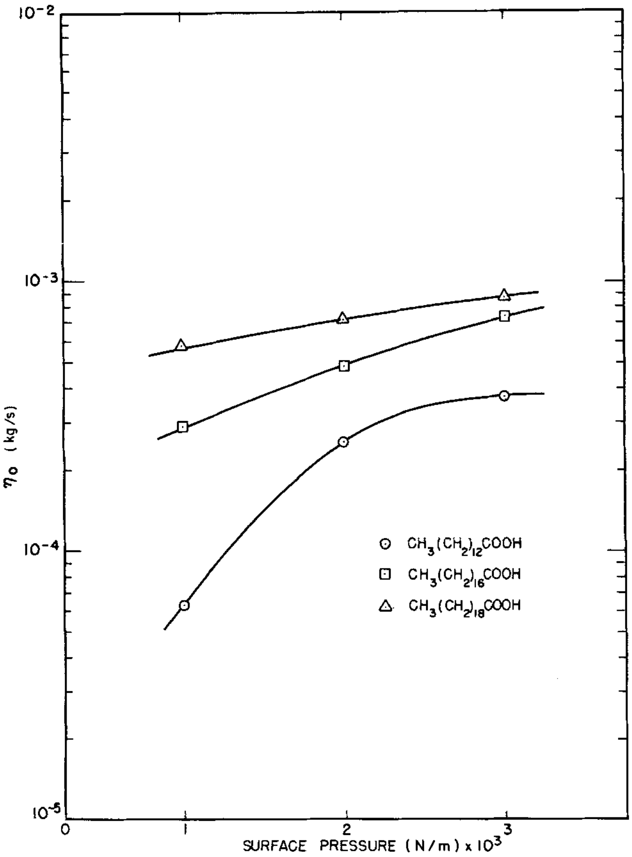

Fig. 11. Zero shear rate viscosity (η_0) vs. surface pressure for C-14, C-18, and C-20 long chain fatty acids spread on a pH 6.1 substrate.

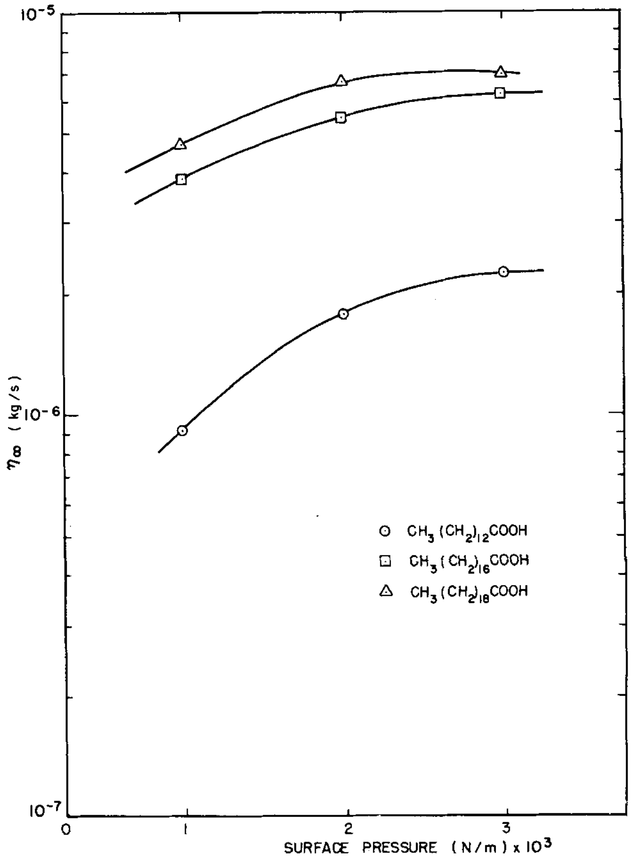

Fig. 12. Infinite shear rate surface viscosity (η_0) vs. surface pressure for C-14, C-18, and C-20 long chain fatty acids spread on a pH 6.1 aqueous substrate.

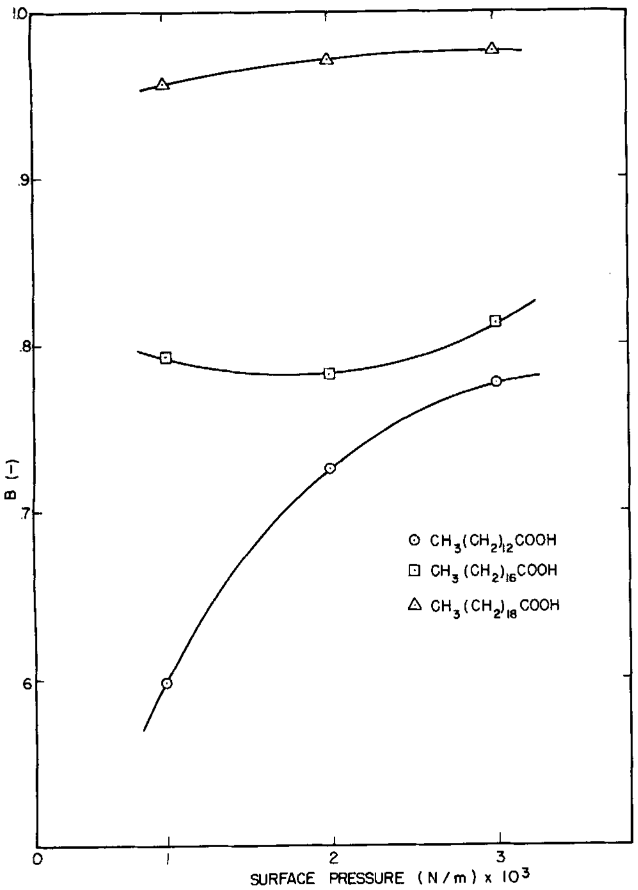

Fig. 13. B vs. surface pressure for C-14, C-18, and C-20 long chain fatty acids spread on a pH 6.1 aqueous substrate.

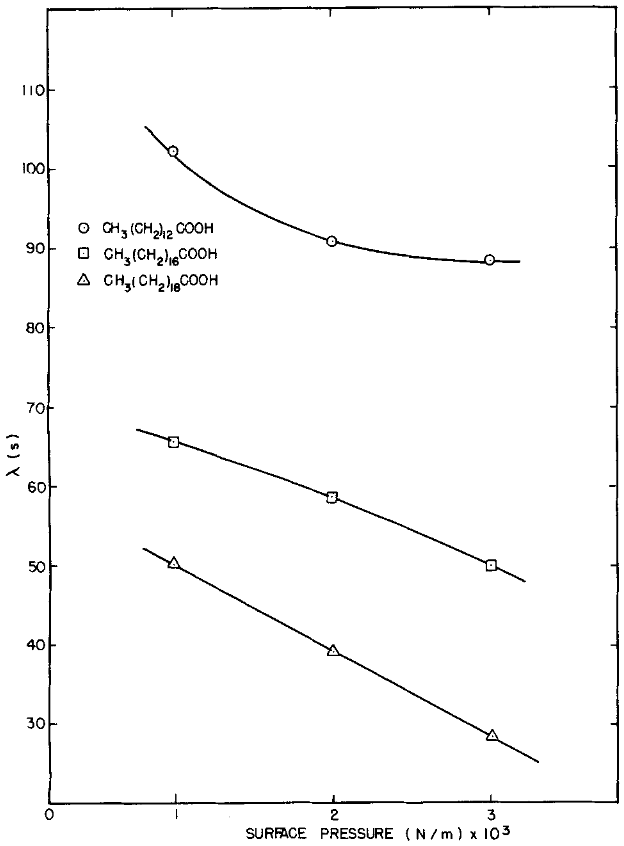

Fig. 14. Relaxation time (λ) vs. surface pressure for C-14, C-18, and C-20 long chain fatty acids spread on a pH 6.1 aqueous substrate.

The remaining parameter λ, or relaxation time, was determined from data obtained from the oscillator experiment. Figures 8, 9, and 10 show the experimental A_p/A_f vs. frequency data for the C-14, C-18, and C-20 acid films, respectively, at film pressures of 0.001, 0.002, and 0.003 N/m.

The experimental data were fit with a regression routine, using the five-parameter model for complex surface viscosity [Equations (16) and (17)].

Owing to the limitation of a relatively narrow frequency range (~0.01 to 2.0 cps), A_p/A_f vs. frequency data required to accurately determine $\eta_0(A_p/A_f \rightarrow 0)$ and $\eta_\infty(A_p/A_f \rightarrow \infty)$ were only partially obtainable. For this reason, the values of η_0 and η_∞ found to best fit the surface viscometry experiment were used in curve fitting the oscillatory data.

For α and β fixed and equal to 2, the parameter λ was determined for each film, and, subsequently, B was calculated from the results of the surface viscometer experiment. Values of the parameters for the three films are given in Table 1.

Generally speaking, the zero shear rate surface viscosity η_0 increases with film pressure and molecular weight (Figure 11). The infinite shear rate viscosity η_∞ follows the same trend; however, the values are smaller by two orders of magnitude (Figure 12). The parameter B varied from 0.60 to 0.98 and was also found to increase with film pressure and molecular weight (Figure 13), although at a much smaller rate than either η_0 or η_∞.

The relaxation time λ decreases with film pressure and molecular weight (Figure 14) which corresponds to a proportional increase in both the viscous (η') and elastic (η'') terms of the complex surface viscosity η^*. In this particular set of experiments, $(\lambda_n\omega)^2 >> 1$ for all n (or frequency, $\omega >> \sqrt{1/\lambda_n}$) so that by Equations (16) and (17), η' and η'' increase with decreasing λ. However, for small frequencies such that $(\lambda_n\omega)^2 << 1$ ($\omega << \sqrt{1/\lambda_n}$), the surface viscosity and elasticity increase with increasing relaxation time.

Effect of Substrate *p*H

In experiments conducted with spread fatty acid films, the *p*H of the substrate was found to have a profound effect upon the surface rheological behavior. Figure 15 shows the experimental T_f/T_p vs. Ω curves for arachidic acid films spread on substrates of various *p*H. (The molecular coverage in all cases was 2.2×10^{-19} m²/molecule.) Typical viscoelastic behavior is observed for the film spread on a *p*H 6.1 substrate, but at *p*H 2.0, it behaves as a Newtonian film with small surface viscosity. At *p*H 4.2, the film appears to be at an intermediate state between the highly viscous and elastic film at *p*H 6.1 and the Newtonian surface at *p*H 2.0. The period ratio data for the film on *p*H 2.0 substrate are difficult to separate from those expected for a film-free interface. In fact, the surface viscosity is too small to be detected using the deep-channel viscometer (the solid line through the data represents the theoretical prediction for the case where no film is present at the interface and $D = 0.1953$). Jarvis (1965) has conducted rheological experiments with fatty acid films on *p*H 2 aqueous substrates using the canal viscometer and has also found that the rheological behavior is Newtonian and that the measured surface viscosities are quite small.

The dissociated acid form, $RCOO^-$, at *p*H 6.1 is much more prevalent than at *p*H 2.0. This may explain the observed rheological behavior. At *p*H 2.0, the acid is apparently present, predominantly in the undissociated form, and hydrogen bonding between the —COOH moieties tends to stabilize the molecular network; however, at *p*H 6.1, the anionic carboxylate ($RCOO^-$) ion concentration is greater, which gives rise to strong charge interactions, and the molecular network can be likened to a fluid crystal. This observation may not completely explain the rigidity of films spread on the *p*H 6.1 substrate. However, studies have been made (Jarvis, 1965; Spink and Sanders, 1955) that show dissociated fatty acids films in the presence of small concentrations of multivalent cations tend to form rigid films of soaps at high substrate *p*H (this phenomenon is due most likely to an intermolecular bridging of $RCOO^-$ anions and M^{+n} cations at the surface). It is possible that small concentrations of cationic species may have been present in the substrate, thereby contributing to the observed *p*H response. It is not possible to distinguish between these two mechanisms without conducting extensive tests.

Experimentally Determined Model Parameters for an Adsorbed Polymeric Monolayer

A polymeric monolayer adsorbed at the air/water interface has been studied using the techniques described in the preceding sections. In this case, the substrate consisted of an aqueous solution of 88% hydrolized poly (vinyl-alcohol) having an average molecular weight of 10 000. The solution concentration was 0.05 wt %, which corresponds to the critical micelle concentration (CMC). The bulk viscosity of this solution was 1.03×10^{-4} N·s/m² under experimental conditions (23 ± 1°C).

After we allowed 8 hr for equilibration by diffusion, data were obtained with the surface viscometer (Figure 16) and the oscillatory rheometer (Figure 17). Note that the limiting period ratio $(T_f/T_p)_\infty$ was unobtainable owing to the excessively high floor rotation rate required. Consequently, data from the oscillatory rheometer were used to determine η_∞. The parameters best describing this film are given in Table 1.

Note that B/λ is roughly twice as large as for the spread films. This can be seen by the fact that the transition rate is higher by a factor of ~2. The higher transition shear rate suggests that molecular interactions, possibly entanglements, are greater in poly(vinyl-alcohol) films than in fatty acid films. This seems plausible, since the entire poly(vinyl-alcohol) molecule is believed to lie lengthwise at the interface, and, furthermore, the molecular weight (or chain length) is much greater than for the fatty acids studied.

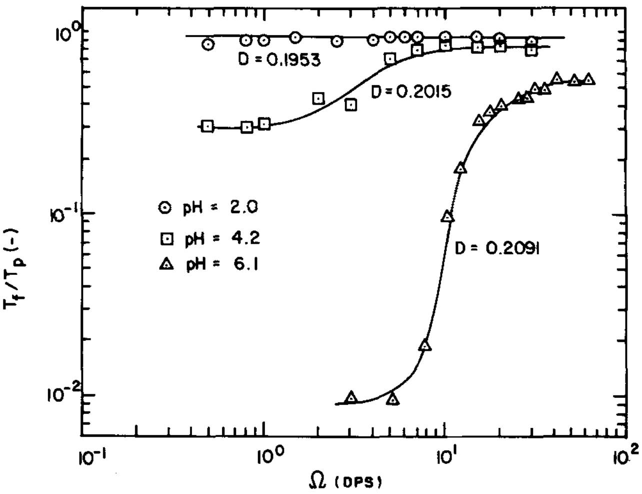

Fig. 15. T_f/T_p vs. Ω for an arachidic acid film spread on a *p*H 2.0, *p*H 4.2, and *p*H 6.1 aqueous substrates.

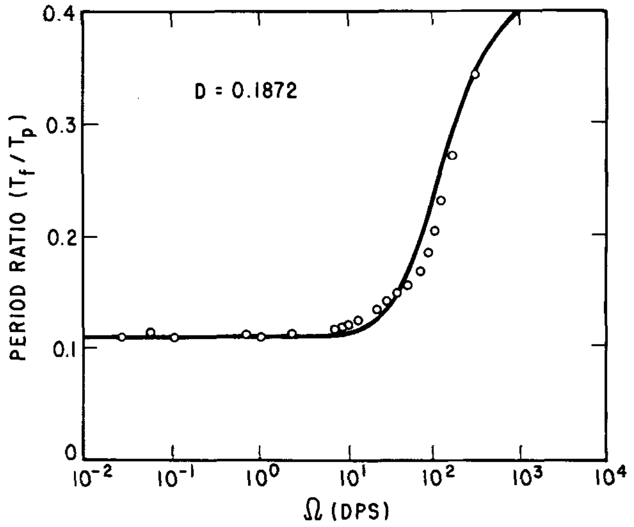

Fig. 16. T_f/T_p vs. Ω for adsorbed poly(vinyl-alcohol) (bulk concentration equal to CMC).

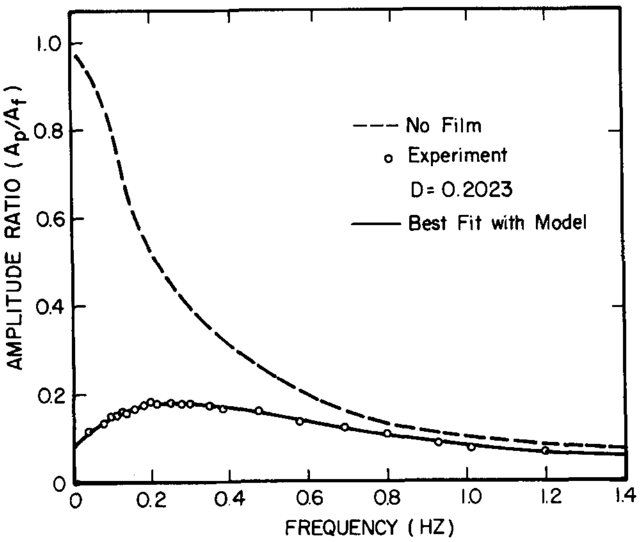

Fig. 17. A_p/A_f vs. frequency for adsorbed poly(vinyl-alcohol) (bulk concentration equal to CMC).

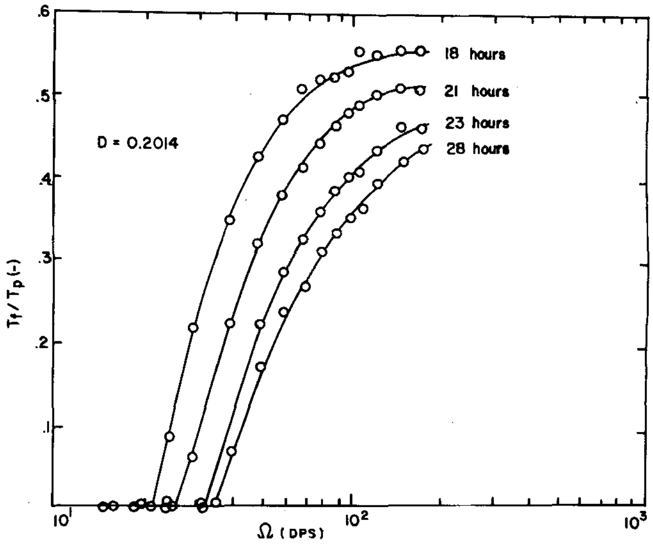

Fig. 18. T_f/T_p vs. Ω for adsorbed poly(vinyl-alcohol) as a function of time (bulk concentration equal to 0.5 ppm).

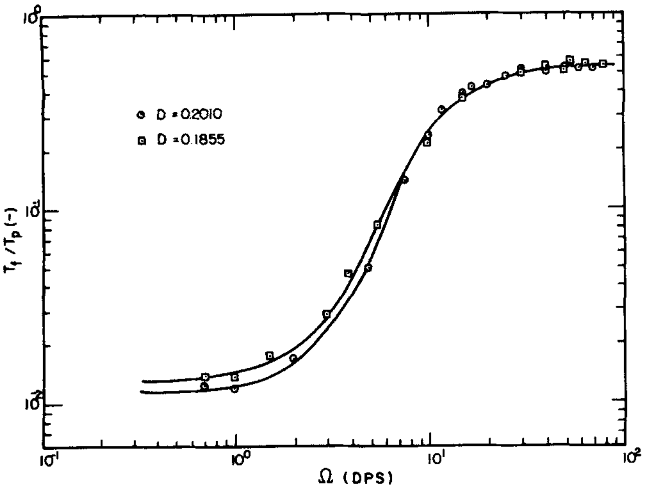

Fig. 19. T_f/T_p vs. Ω for a stearic acid film spread on a pH 6.1 aqueous substrate ($\pi = 0.002$ N/m) at two values of D.

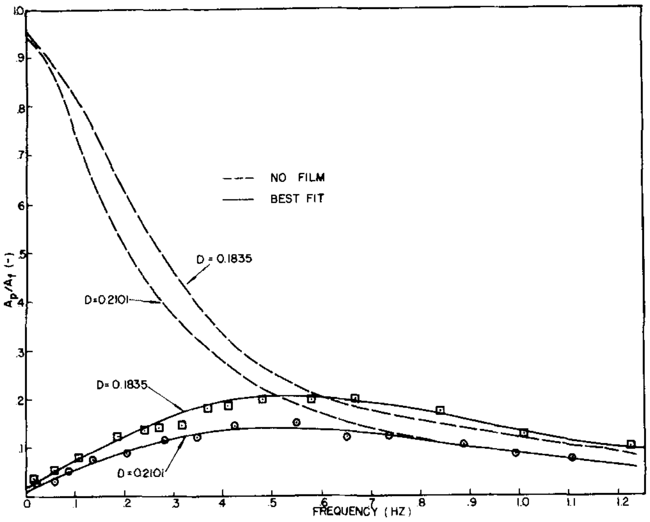

Fig. 20. A_p/A_f vs. frequency for a stearic acid film spread on a pH 6.1 aqueous substrate ($\pi = 0.002$ N/m) at two values of D.

Time Dependent Behavior

Time dependent rheological behavior has been observed for an adsorbed film of high molecular weight poly(vinyl-alcohol). In these experiments, the substrate consisted of an aqueous solution of 100% hydrolyzed poly(vinyl-alcohol) having an average molecular weight of 115 000. The solution concentration was 0.5 ppm.

Figure 18 shows the period ratio vs. floor speed curves for this film at various times before the film equilibrated. The behavior here for any particular curve is similar to that observed for the fatty acid films, except that the film was completely rigid at low floor speeds, and the limiting period ratio $(T_f/T_p)_\infty$ was obtained only at excessively high floor speeds (because the maximum allowable floor speed was exceeded, a detailed numerical analysis could not be justified).

TABLE 3. EXPERIMENTALLY DETERMINED η_∞ FOR A TETRADECANOIC ACID FILM ($\pi = 0.004$ N/M) AT THREE VALUES OF D

D	$(T_f/T_p)_\infty$	η_∞(kg/s)
0.2336	0.610	2.9×10^{-6}
0.1996	0.708	2.6×10^{-6}
0.1339	0.797	3.0×10^{-6}

The apparent yield stress (which may be related to the transition floor speed) and η_∞ both increase with time up to 28 hr, after which time it was found that the film had equilibrated and no further changes in period ratio were observed. The behavior illustrated by this film is believed to be due to a slow surface-diffusion rate in which the concentration of poly(vinyl-alcohol) molecules at the surface steadily increases and approaches an equilibrium value.

Sensitivity

The experimentally determined parameters α, β, λ, η_0, η_∞, and B should, in theory, be independent of the experiment used to determine them. In particular, the value of the operational parameter D used in the experiment should not affect the values of the parameters. In practice, however, the parameters obtained from experiments may be sensitive to the depth of fluid in the canal (depth = $y_0{}^*D$). This would indicate either a failure of the model in the case of large differences or simply experimental error for small deviations.

To determine this sensitivity to D, experiments were performed at two different depths for a spread stearic acid film ($\pi = 0.002$ n/m). Figures 19 and 20 show the experimental data, and Table 2 lists the parameters giving the best fit. Although the two parameter sets differ only by approximately 10%, it is clear that some modifications of the apparatus design is necessary before this surface rheological technique can be considered analytic.

In some experiments, the floor speed was as high as 75 deg/s (see Figure 7), which is greater than the apparent maximum allowable floor speed for $D \doteq 0.2$. Such high floor speeds were necessary to determine the limiting period ratio $(T_f/T_p)_\infty$. It is possible that the limiting period ratios thus obtained may be artifacts due to secondary surface flows. To test this hypothesis, $(T_f/T_p)_\infty$ data were measured for three different depths using a tetradecanoic acid film ($\pi = 0.004$ n/m). In addition, the maximum floor speed used (70 deg/s) was in excess of the apparent maximum allowable speed for any value of D. The limiting period ratios and corresponding surface viscosities (η_∞) for the three depths are given in Table 3.

The relatively good agreement between the calculated surface viscosities in the high shear rate range (defined by $D = 0.1339$) and the low range ($D = 0.2336$) indicates that secondary flow is not a large source of error even at floor speeds as high as 70 deg/s, provided the surface viscosity (η_∞) is greater than ~3×10^{-6} kg/s. This tends to support the assumption that secondary flows are damped out by viscous surfaces.

TABLE 2. SENSITIVITY OF EXPERIMENTALLY DETERMINED PARAMETERS TO D

	D	η_0 (kg/s) $\times 10^3$	η_∞ (kg/s) $\times 10^3$	$B/\lambda(s^{-1})$	$\lambda(s)$	$B(-)$
Viscometric experiment	0.2010	0.4820	0.00543	0.0133	—	0.7820
	0.1855	0.5340	0.00610	0.0133	—	0.8366
Oscillatory experiment	0.2101	—	—	—	58.8	—
	0.1835	—	—	—	62.9	—

$\alpha = \beta = 2.0$.

NOTATION

A_p/A_f = amplitude of surface center-line oscillation/amplitude of floor oscillation
B = model parameter related to the amount of deformation at which the surface loses its memory (see Gardner, 1975)
D = ratio of depth to annular spacing
G' = dynamic surface rigidity
i = $\sqrt{-1}$
$Im\{\ \}$ = imaginary part of $\{\ \}$
$m(s)$ = memory function
s = time into the past
t = time
T_f/T_p, $(T_f/T_p)_0$, $(T_f/T_p)_\infty$ = period of floor rotation/period of surface center-line rotation; period ratios for $\dot{\gamma} \to 0$ and $\dot{\gamma} \to \infty$, respectively
V^* = complex velocity function
y = radial distance from inside wall of canal
y_0 = annular spacing in canal

Greek Letters

α = model parameter
β = model parameter
$\delta(s)$ = dirac delta function
$\dot{\gamma}$ = surface shear rate magnitude
$\eta(\dot{\gamma})$ = steady shear surface shear viscosity
η^* = complex surface viscosity
η' = dynamic surface viscosity (real part of η^*)
η'' = imaginary part of η^*
η_0 = zero shear rate surface viscosity
η_∞ = infinite shear rate surface viscosity
λ = relaxation time
π = surface pressure
Ω, Ω_{max} = floor rotation rate, maximum allowable rotation rate
ω = frequency

ACKNOWLEDGMENT

The authors wish to express their appreciation to the Department of Health, Education and Welfare and El Paso Products Company for providing financial assistance to J. V. Addison.

LITERATURE CITED

Addison, J. V., "An Experimental Study of the Rheological Behavior of Surface Films," M.S. thesis, Department of Chemical Engineering, Univ. Tex., Austin (Dec., 1977).

Bird, R. B., and P. J. Carreau, "Nonlinear Viscoelastic Model for Polymeric Solutions and Melts," *Chem. Eng. Sci.*, **23**, 427 (1968).

Burton, R. A., and R. J. Mannheimer, "Analysis and Apparatus for Surface Rheological Measurements," *Adv. Chem. Ser.*, **3**, 315 (1967).

Gardner, J. W., "On the Mechanics of Non-Newtonian Films," Ph.D. dissertation, the Univ. Tex., Austin (1975).

———, J. V. Addison, and R. S. Schechter, "A Constitutive Equation for a Viscoelastic Interface," *AIChE J.*, **24**, 400 (1978).

———, and R. S. Schechter, "Evaluation of Surface Rheological Models," *J. Colloid and Interface Science, Vol. IV: Hydrosols and Rheology*, p. 421, Academic Press, New York (1976).

Jarvis, N. L., "Surface Viscosity of Unimolecular Films of Long-Chain Aliphatic Amides, Alcohols and Carboxylic Acids," *J. Phys. Chem.*, **69**, No. 6, 1789 (1965).

Mannheimer, R. J., "Non-Newtonian Properties of Surface-Active Materials," Ph.D. dissertation, Univ. Tex., Austin (1968).

———, and R. S. Schechter, "The Theory of Interfacial Viscoelastic Measurements by the Viscous Traction Method," *J. Colloid Interface Sci.*, **32**, No. 2, 224 (1970).

Pintar, A. J., A. B. Israel, and D. T. Wasan, "Interfacial Shear Viscosity Phenomena in Solutions of Macromolecules," *ibid.*, **37**, 52 (1971).

Spink, J. A., and J. V. Sanders, "Soap Formation in Unimolecular Films on Aqueous Solutions," *Trans. Faraday Soc.*, **51**, 1154 (1955).

Tanner, R. I., and J. M. Simmons, "Combined Simple and Sinusoidal Shearing in Elastic Liquids," *Chem. Eng. Sci.*, **22**, 1803 (1967).

Manuscript received November 22, 1977; revision received August 11 and accepted August 25, 1978.

Applications of a Stretch Model to Mixing, Diffusion, and Reaction in Laminar and Turbulent Flows

WILLIAM E. RANZ

**Department of Chemical Engineering
and Materials Science
University of Minnesota
Minneapolis, Minnesota 55455**

In a Lagrangian frame of reference based on lamina (fluid filament) thickness and in a warped time scale based on a single, flow dependent quantity, mixing, diffusion, and reaction can be described in a relatively simple way. Applications are presented for stretch and fold in taffy pull, egg beater and static mixer, shear stretch, stretch of laminae in a vortex, mixing with diffusion, reaction rate controlled by diffusion of reactant through a product layer, and very fast reactions in a turbulent flow.

SCOPE

Mixing, diffusion, and reaction of soluble fluids have been analyzed primarily in a fixed frame of reference and in terms of the statistical descriptions and theories of fluid mechanics or in terms of variables of distributed value such as residence time. The objective here is to introduce in terse form a type of description and analysis which results in deterministic and predictive models capable of extensive application and development, and to demonstrate use with brief examples.

0001-1541-79-1892-0041-$00.95.